CHAPTER 3

The role of electron donating and electron withdrawing groups in tuning the optoelectronic properties of difluoroboron-napthyridine analogs

Abstract

Five napthyridine based fluorine-boron (BF_2-napthyridine) conjugated compounds have been theoretically designed, and subsequently, their photophysical properties are investigated. The influence of electron donating and electron withdrawing groups attached with the N^C^O moiety of BF_2-napthyridine molecule has been interpreted. The optoelectronic properties, including absorption spectra and emission spectra of the BF_2-napthyridine derivatives are studied using density functional theory (DFT) and time-dependent density functional theory (TD-DFT) based methods. Different characteristics, such as, HOMO-LUMO gap, molecular orbital density, ionization potential, electron affinity, reorganization energy for hole and electron are calculated. All these molecules show excellent π-electron delocalization. TD-DFT results illustrate that amine substituted BF_2-napthyridine derivative has highest absorption and emission maxima, it also shows maximum Stoke shift. These results are well correlated with the structural parameters and calculated HOMO-LUMO gap. Moreover, it is found that, introduction of electron donating group into the BF_2-napthyridine complex improves the hole transport properties and provides useful clues in designing new materials for organic light emitting diode (OLED). As a whole, this work demonstrates that electron donating and electron withdrawing groups in BF_2 derivatives can extend their effectiveness towards designing of OLED materials, vitro cellular studies, ex vivo assays, and in vivo imaging agents.

3.1. Introduction

Boron containing complexes are known to exhibit extraordinary optical properties.[1,2] Their astonishing characteristics have attracted considerable interest among researchers due to their prevalent application in various fields.[3] Optical properties of fluorescent boron difluoride (BF_2) are tuneable through structural modification which enhances their properties towards new applications. The π-conjugation skeleton of BF_2 complexes as in O, O- ; N, O- ; N, N- chelating ligands (Scheme 3.1) are very important for implementation in organic electronics with high electron affinities and mobilities.[4-9]

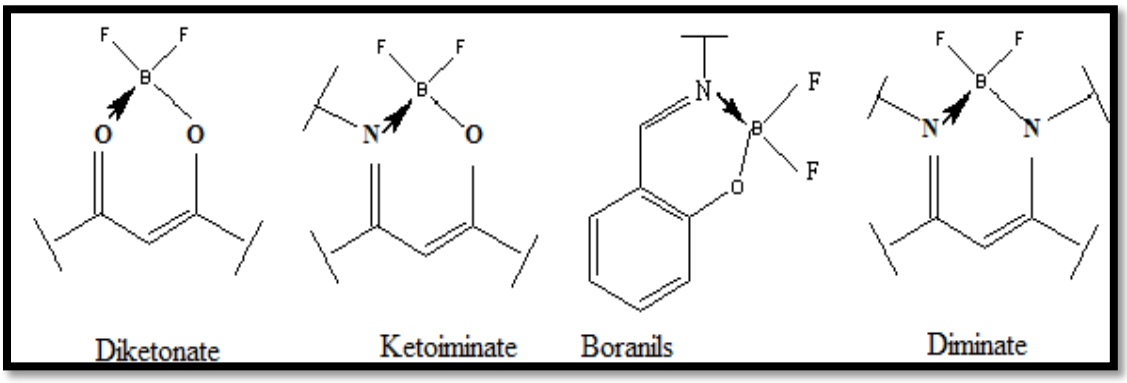

Scheme 3.1. Basic types of difluoroboranyl complexes.

One of the easiest methods for adjusting spectral properties is to modify the substituents which persuade the electronic distribution.[10,11] Delocalization of electron over the π-conjugation skeleton made boron complexes highly fluorescent and thermally stable.[12,13] Therefore, fluorescence property can be enhanced by increasing π-conjugation in molecules.[14,15] It is reported that π-conjugated polymers have high charge carrying properties which make them significant materials for evolution of new opto and/or electronic devices like photovoltaic cell,[16] organic light emitting diode (OLED)[17] etc. One of the most common examples of BF_2 complex is boron dipyromethane (BODIPY) which holds remarkable photo-physical and photochemical properties. These types of molecules can be used as sensing and imaging agents due to their high fluorescence quantum yields in the visible region.[18,19] Furthermore, difluoroboron complexes can be

used in optoelectronic device[20-22] and potential photosensitizers in dye-sensitized solar cell.[14],[23],[24] A recent report demonstrates that boron complex bearing a pyrene ligand shows potential application in OLED.[25] Light emitting materials prepared by controlled synthetic method are much beneficial for biological imaging and sensing. It is known that optical properties of difluoroboron dibenzoylmethane poly (lactic acid) can be used in live cell imaging for cellular uptake and trafficking studies.[26]

Napthyridine derivatives can be used as ligand for BF_2 complexes because of their good fluorescence properties and biocompatibility.[27-29] This class of compounds have been reported to be used in chemotherapy.[30] Different types of 1, 8-napthyridine derivatives also show potential antibacterial activities.[31],[32] These molecules possess heterocyclic moiety which is an attractive tool for identification of novel potential antitumor agents and also have high medicinal values.[33] Roma et al. synthesized novel 1, 8-napthyridine-3-carboxamide derivatives, [1,2,4] triazole [4,3-a] [1,8] napthyrin derivatives which reveal high anti-inflammatory activities along with substantial anti-aggressive properties.[34] Some novel compounds of napthyridine derivatives also hold high fluorescence quantum yield. Through H-bonding, N atom in this compound can efficiently bind with nitrogenous base of DNA. Teramae and co-workers demonstrated that, 2-amino-5, 6, 7-trimethyl-1, 8-napthyridine (ATMND) exhibits drastic quenching in fluorescence intensity upon pseudo base pairing with a cytosine residue in an oligonucleotide duplex.[35],[36] A previous report confirmed that 1, 8-naphthyridine derivative with pyrrole moieties can be used to sense sugars through changes in absorption and fluorescence. These compounds also show low toxicity.[37],[29] A newly synthesised bis(5,7-dimethyl-1,8-naphthyridin-2-yl)amine, has been reported to show fluorescence property.[38] Recently, Li et al. have synthesized 1,2-bis(5,7-dimethyl-1,8-naphthyridin-2-yl)hydrazine complex which is highly fluorescent and exhibits yellow-green emission with high quantum yield.[39]

To the best of our knowledge, there has been no report about the influence of electron donating or withdrawing groups into difluoroboron napthyridine (BF_2-napthyridine) fragment. The search of alternative fluorescent compound encourages us to envisage changes in the nature of BF_2 chelating moiety. In the present work, we design

some novel organic fluorine-boron compounds containing amine substituted 1, 8-naphthyridine complex and compute the absorption and emission spectra both in vacuum and in dichloromethane (DCM) solvent using the TD-DFT method. Fig. 3.1 depicts novel difluoroboron napthyridine compounds (A to E) and their numbering scheme. Position 4 of 1,8-napthyridine moiety is substituted with amino group because it is known that the presence of auxochromes can shift the colour of a dye and influence the solubility.[40] We choose DCM as an example of polar solvent for the purpose of comparison. The main idea is to obtain the structure with an electron donating or electron withdrawing group attached with the N^C^O moiety of BF_2 and to check how the binding of electron donating and electron withdrawing groups on BF_2 influence the spectral properties of the molecule. To achieve more information, ionization potential (IP), electron affinity (EA) and reorganization energy of holes and electrons are calculated to explain the transport phenomenon. Thus, the development of red-shifted BF_2 derivatives can extend their effectiveness towards designing of OLED materials, vitro cellular studies, ex vivo assays, and in vivo imaging agents.

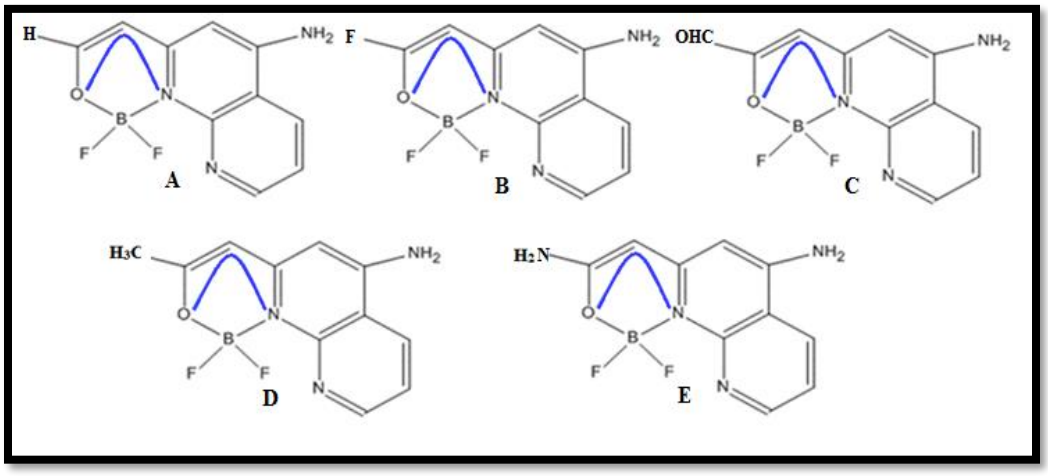

Fig. 3.1. Proposed structure of napthyridine fused difluoroboron compounds. Blue colour denotes N^C^O moiety.

3.2. Computational Details

All computations were performed using Gaussian 09 programme package[41] at B3LYP/6-311+G(d) level of theory[42] otherwise stated elsewhere. Geometry optimization was carried out in the gas phase and in solution phase by applying polarizable continuum model (PCM) without symmetry constraints. Tolerance limit during optimization has been set as 10^{-8} a.u. The vibrational frequencies of the optimized structures were computed by using same functional and basis set to characterize the nature of stationary states. The absorption and emission spectra were characterized by time-dependent (TD) density functional theory (DFT), specifically TD-B3LYP, in a more flexible basis, 6-311+G (d). The absorption band (i.e., $S_0 \rightarrow S_1$ transition) and emission band (i.e., $S_1 \rightarrow S_0$ transition) were calculated in the gas phase and in DCM. The vertical excitation energies and oscillator strengths were obtained for the lowest 6 singlet – singlet transitions of the optimized ground state by using the TD-DFT at the same level of theory. The low-lying first singlet excited states (S_1) of these five compounds were relaxed using the TD-DFT to get their minimum energy geometries.

The vertical emissions were obtained by using this optimized relaxed singlet first excited state geometry. All the computations in gas phase and in solvent were carried out using the Self-Consistent Reaction Field (SCRF) incorporated in the Polarizable Continuum Model (PCM).[43],[44] The absorption spectra, including wavelengths, oscillator strengths, and main configuration assignment, were systematically investigated using TD-DFT on the basis of the optimized structures. To understand the electronic transitions occurring in the molecule, isodensity plots of the frontier molecular orbitals were generated with GaussView 5.0.

3.3. Results and Discussions

3.3.1. Structural parameters

The difluoroboron-napthyridine analogs having a central difluoroboron core is coordinated to the end of N and O atoms of the N^C^O chelating group is shown in Fig.

3.1. The optimized geometries of proposed BF_2-napthyridine compounds are given in Fig. S1 (Supporting information). The structural differences of the compounds between the ground state and excited state geometry by the $S_0 \rightarrow S_1$ transition can be illustrated by scrutinizing the extent of bond length variation (Supporting information, Fig. S2 and Table S2 to S6). In complex A to E, the C-O bond length in the boron containing ring are between typical C-O (ca. 1.43Å) and C=O (ca. 1.23Å) bond lengths. For all complexes the B-N and B-O bond lengths are in the range 1.556 - 1.639 Å and 1.476 - 1.573 Å in ground and excited state for both phases. The B-O bond lengths are considerably smaller than the B-N bond length. These results indicate that the BF_2 containing six membered rings have delocalized iminoenolate structure. Those values are comparable to the reported difluoro(amidopyrazinato O,N) boron derivatives.[45] Further it has to be noticed that a major increment in bond length parameter (>0.05 Å) observed in the following cases: a) B-O bond length for compound A, D and E and b) non-fused C-C bond length in boron containing ring for compound A and D, NH_2 substituted napthyridine moiety in compound B and E. The increase in B-O and C-C bond lengths can be rationalized by consideration of the nodal structures of the HOMO and LUMO orbitals in Fig 3.6 and Fig. S3, S4 and S6 in supporting information. The lowest energy $S_0 \rightarrow S_1$ transition is mainly HOMO $\rightarrow$ LUMO in character. There are nodes across the C-C bonds in the LUMO orbitals, while the HOMO orbital has bonding character and as a result the elongation of these bond lengths occurs. In compound C, decrease in 14C-25C bond length found which suggests that partial double bond character grows in excited state geometry. All the compounds in ground state and in excited states are very nearly planar (Fig. S2 and Table S3 to S11, shown in supporting information). When the geometries of compounds in gas phase and in DCM are compared, it has been found that solvated systems show more planarity than gas phase. N atom of amino group is lying on the plane of the napthyridine ring to which the amino group is attached. Some selected bond parameters obtained from the optimized geometries of BF_2–napthyridine derivatives are depicted in Fig. 3.2 and in Supporting information, Fig. S2. We notice that bond angles which are mentioned in Fig. 3.2 moves to more planar region in excited state compared to the ground state in case of electron donating substituents D and E. All the dihedral angles (φ_1, φ_2, φ_3, φ_4 and φ_5) in Fig. 3.2 are nearly planar, in ground state as well as in excited

state. All these calculated parameters indicate that these five molecules have an excellent π-electron delocalization throughout the molecule. It is important to remember that delocalization is one of the main features to get excellent optoelectronic properties. The ground state dipole moment of all the molecules in the vacuum are in the range of 8.9194 D to 13.8684 D and in the DCM are in the range of 9.5606 D to 15.8249 D, which indicate that in the solvent phase molecules get stabilized by the medium (Supporting information, Table S12). So, these results conclude that the dipole moment is increased in the polar medium approximately by 10%. The enhancement of dipole moments in polar solvent compare to gas phase is a natural consequence of the stabilization by the medium. The unsymmetrical charge distribution in DCM is more than that in the gas phase. The calculated molecular energies of BF_2 co-ordinated N^C^O functional group of compound A-E in gas phase and in DCM are given in Table S13.

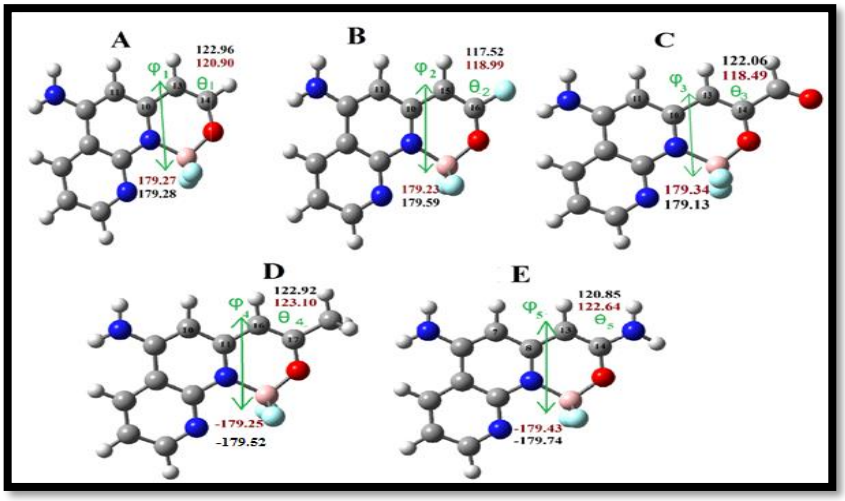

Fig. 3.2. Selected bond parameters obtained from the optimized geometries of BF_2–napthyridine derivatives. Note: φ indicates dihedral angles (φ_1 = C11–C10–C13–C14; φ_2 = C11–C10–C15–C16; φ_3 = C11–C10–C13–C14, φ_4 = C10–C11–C16–C17; φ_5 = C7–C8–C13–C14); and θ indicates bond angles (θ_1 = C13–C14–H, θ_2 = C15–C16–F, θ_3 = C13–C14–CHO, θ_4 = C16–C17-CH_3, θ_5 = C13–C14–NH_2). Brown colour denotes parameters of the ground state and black colour depicts parameters of the excited state. All data provided in the figure are in gas phase.

3.3.2. Effect of solvent polarity in the dipole moment

For the difluoroboron-napthyridine complexes it is found that the ratio of ground state to excited state dipole moment is greater than one. For difluoroboron napthyridine molecules, the dipole moment values range from 9.5606 D to 15.8249 D for ground state and 11.8784 D to 20.4670 D for excited state in DCM (Table S14, provided in supporting information). This clearly suggests that compounds are more polar in excited state and stabilized by the polar solvent environment which is also reflected in structural parameters. Dipole moment values demonstrate that compound C has better push-pull ability both in the ground and in the excited states compared to A. For all the compounds push-pull ability is stronger in the excited state than in the ground state. We can further predict that, the electronic properties of compounds can be easily influenced by the solvent environment.

3.3.3. Absorption properties

To understand the electronic properties of napthyridine based compounds, the vertical excitation energies were recorded with TD-DFT method and labelled in Table 3.1. It has been found from Table 3.1 that all electronic transitions are $\pi \rightarrow \pi^*$ type among the calculated singlet-singlet transition and oscillator strength for $S_0 \rightarrow S_1$ transition is attributed to HOMO → LUMO transition for all compounds with maximum absorption whereas HOMO−2 → LUMO transitions are obtained with weak oscillator strength. In the case of compound D, it has been observed that by substitution of electron donating methyl group into the difluoroboron chelating moiety, the absorption wavelength increases by only 4 nm. Moreover, the presence of a lone pair of electrons in the Nitrogen atom of NH_2 substituted compound in E influences the absorption energy more, subsequently the absorption wavelength increases by 12 nm. Therefore, as the conjugation is strengthen the wavelength of absorption maxima increases. For all the molecules, the dominant absorption band observed to be associated with the difference of highest occupied molecular orbital (HOMO) to the lowest unoccupied molecular orbital

(LUMO). The above results reveal that substitution of electron donating groups to the BF_2-napthyridine core shifts the absorption spectrum towards the higher wavelength region. The UV-Visible absorption spectra (Fig. 3.3.a) of compounds in gas phase show maxima in two separated regions (Table 3.1). In general, the shape of the absorption spectrum, the position of its maxima and intensity can be modified with increasing π–conjugation between the difluoroboranyl unit and the electron donating group.

The UV-Visible spectra of A-E complexes in gas phase show strong band at 364 nm, 356 nm, 373nm, 368 nm and 376 nm with a shoulder in between 306 nm - 323 nm. Absorption band at 356 -376 nm is assigned to the π-π* transition due to the presence of the conjugated napthyridine moiety in the architecture (Table 3.1). It is worth to mention that the absorption bands display a moderate red shift on moving from B, A, D, C and E and chronologically. This is due to the increasing donor strength on the molecule.[46] Exception in case of compound C found in vacuum, which may be due to the extending conjugation of –C=O group with the rest of the conjugated molecule more rather than –F substituted and methyl substituted BF_2-napthyridine compounds. The computed vertical excitation values of all complexes show red shift in DCM compared to gas phase (Fig. 3.3.b). This can be attributed to the lowering the energy of HOMO-LUMO gap in the polar solvent, as polar solvent stabilized the LUMO orbital more than the HOMO orbital which explained the solvatochromic behaviour of the compounds which is discussed more precisely in the Frontier molecular orbitals section. For all compounds in solution phase absorptions are mostly attributed to HOMO-LUMO transition. For each complex HOMO-LUMO orbitals are nearly delocalized. The observed red shift is in accordance with the theoretical studies which may be due to the smaller HOMO-LUMO energy gap in more polar solvent. Excited states for all molecules show a dominant $\pi \rightarrow \pi^*$ transition from HOMO to LUMO. The optical properties of these compounds were studied in DCM because these condition do not result boron-ligand dissociation[47] or photochemical reaction.[48],[49]

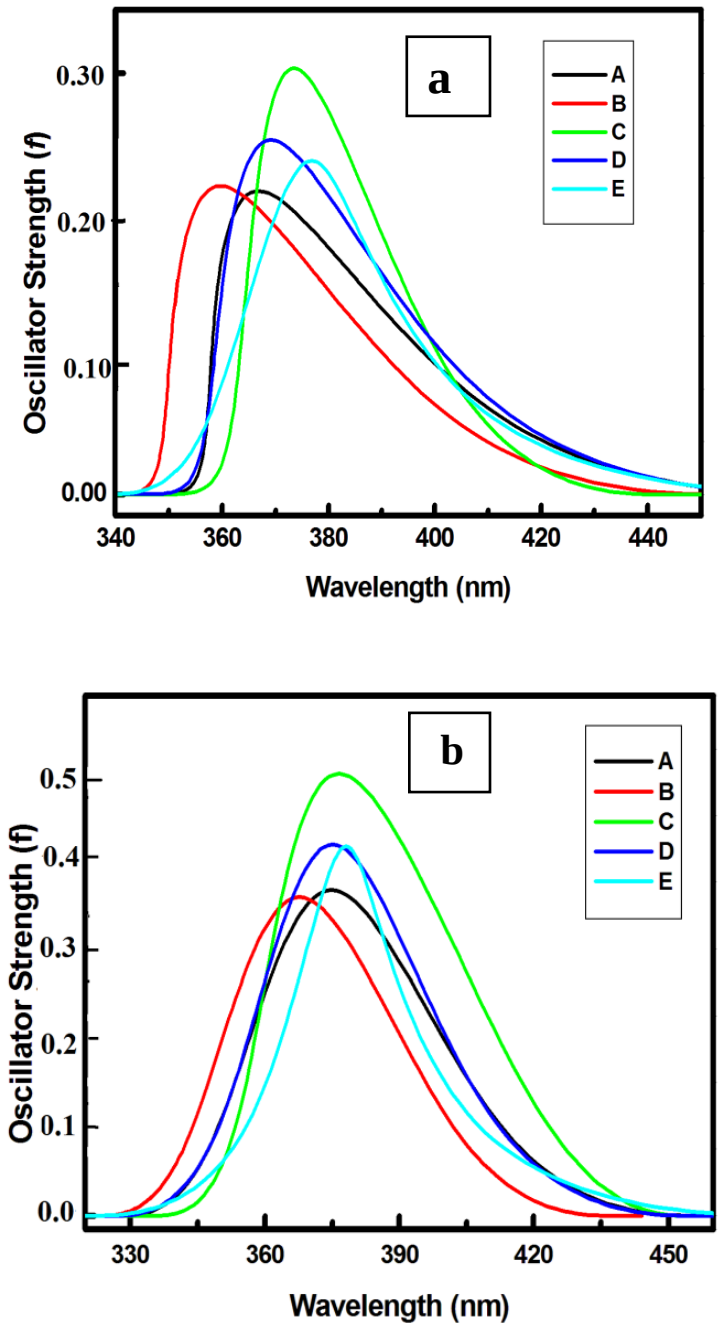

Fig. 3.3. Computed absorption spectra (a) in gas phase and (b) in DCM recorded with TD-B3LYP/6-311 + G (d).

Table 3.1. Calculated maximum absorption wavelengths (in nm), the oscillator strength (*f*), orbital contribution, and excitation energies (in eV) with TD-B3LYP/6-311+G (d) for difluoroboron napthyridine molecule in gas phase and in dichloromethane solvent.

Compounds	Vertical excitation (nm) (TD-DFT)	Excitation Energy (Cm^{-1})	Oscillator strength (*f*)	Orbital Contribution (HOMO-LUMO)	
A(Gas)	364 (3.4091 eV) 318 (3.9029 eV)	27,496	0.216 0.001	H→L H−2→L	0.6888 0.6945
A(DCM)	372 (3.3735 eV)	26,925	0.366	H→L	0.6551
B(Gas)	356 (3.4845 eV) 310 (3.9934 eV)	28,104	0.219 0.001	H→L H−2→L	0.6427 0.6845
B(DCM)	365 (3.3989 eV)	27,395	0.358	H→L	0.6952
C(Gas)	373(3.3229 eV) 323(3.8372 eV)	26,801	0.303 0.003	H→L H−2→L	0.6283 0.5104
C(DCM)	374(3.3119 eV)	26,713	0.501	H→L	0.6982
D(Gas)	368 (3.3735 eV) 316 (3.9282 eV)	27,209	0.252 0.001	H→L H−2→L	0.6900 0.6940
D(DCM)	376 (3.2745 eV)	26,411	0.418	H→L	0.6566
E(Gas)	376 (3.2759 eV) 307 (4.0441 eV)	26,466	0.238 0.001	H→L H−2→L	0.6871 0.6925
E(DCM)	379 (3.2329 eV)	26,023	0.415	H→L	0.6533

3.3.4. Emission spectra

Based on the excited state optimized geometries, the emission energy was computed using time-dependent (TD) density functional theory (DFT) method. The corresponding oscillator strength, orbital contributions are summarized in Table 3.2 and the computed emission spectra are shown in Fig. 3.4. Like absorption spectrum, the emission band is found to be associated with the electronic transition between HOMO and LUMO exception found in case of –F substituted complex in DCM. An analysis of the TD-DFT wave function shows that in case of –F substituted complex, S_1 state corresponds to the HOMO-1 →LUMO transition with large oscillator strength. In this complex, S_1 state has ππ* character in gas phase and nπ* character in solution phase. In DCM, HOMO-1is an n-type orbital, where electron density mainly located adjacent to the F atom of the molecule.(shown in supporting information, Fig. S7) The emission band of A, B, C, D and E compounds in gas phase are observed at 400 nm, 420 nm, 416 nm, 421 nm and 455 nm respectively. Increase in emission wavelength occurs due to the increase in π-conjugation with the BF_2 chelating moiety, electron density delocalization on the frontier molecular orbital and the influence of electron donating substituents, methyl and amino groups. Compound E was found to have a higher λ_{max} in emission.

The studied napthyridine based difluoroboron compound exhibit bathochromic shift in polar DCM solvent ranging from 2.0249 eV to 2.9422 eV. From Table 3.2 (Emission), it has been found that bathochromic shift in the studied molecules is in the increasing order from decreasing electron accepting strength to electron donating ability as A <C <B < D < E in vacuum as well as in DCM. The largest bathochromic shift was found for E in polar solvent about 3.2329 eV and 2.0249 eV in absorption and emission spectra.

It has been observed that the oscillator strength (*f*) increases with the substitution of donor and acceptor groups. NH_2 substituted complex (compound E) show $S_0 \rightarrow S_1$ transition with a large Stokes shift suggests that there is a considerable charge transfer character of the excited state. Theoretically large Stokes shift is found mainly for the intramolecular charge transfer in the molecule[11] although the solvent effect is highly

significant. Marcus theory is used to account for the charge transfer integral. The lower the reorganization energy, higher the charge transfer rate and mobility. We have calculated reorganization energy which is discussed latter in the reorganization energy section. It has been found that $–NH_2$ substituted complex shows lowest reorganization energy value among all the systems thus showing highest charge transfer integral. Remarkable red shift in both absorption and fluorescence maxima suggest charge transfer character in compound E. However, it is worth noting that, the effect of solvent on the shape of emission spectra (Fig. 3.4) is quite significant. From Fig. 3.4 it is clear that in the gas phase, emission spectrum is sharp in nature while in DCM, the spectra get broadened. So, a significant solvatochromic shift is observed. Spectral broadening is dominated by interactions with the solvent molecules and lines are much wider compared to gas phase spectra. Polar solvent perturb the electronic state of a molecule. In the solvent phase, for every molecule, the lifetime is reduced (Table 3.2) due to the increase in the number of collisions. Shorter the lifetime of the states involved in a transition, large uncertainty in the energy occurs, which leads to broadening of the consequent spectral line. In polar environment, as HOMO-LUMO gap decreased, transitions occur with much low energy. Therefore, broadening of the half band width occur. More importantly, the Stokes Shift, the difference between $\lambda_{\max}^{\text{emission}}$ and $\lambda_{\max}^{\text{absorption}}$ for compounds A, B, C, D and E in gas phase are 36 nm, 64 nm, 43 nm, 53 nm and 79 nm and in DCM are 49 nm, 94 nm, 65 nm, 87 nm and 98 nm, respectively. With increasing π conjugation and π donation ability, Stokes shift increases.

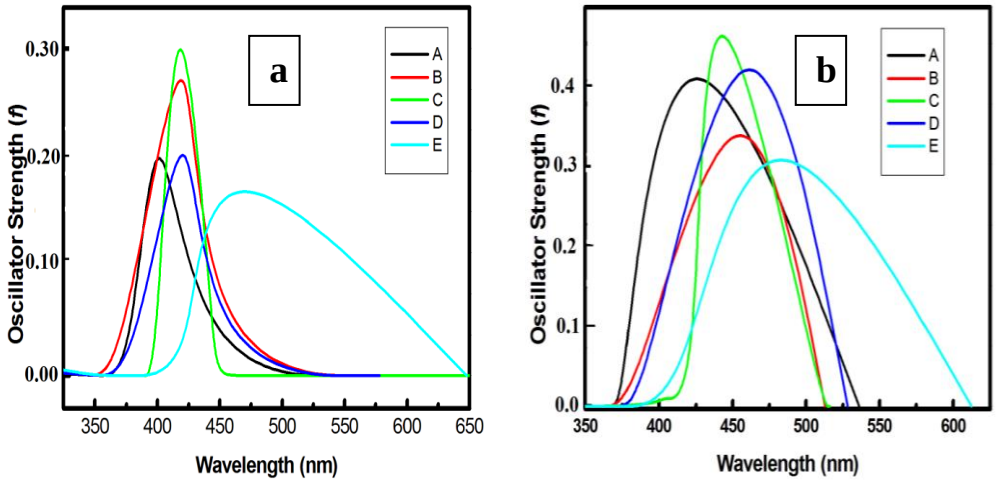

Fig. 3.4 Computed emission spectra with TD-B3LYP/6-311+ G (d) (a) in gas phase and (b) in dichloromethane solvent (DCM) of difluoroboron napthyridine molecule.

In optoelectronics, it is important to know about the radiative life time. The shorter the radiative life time (τ), the better is the light emitting efficiency. The radiative life time can be calculated using the following formula.[50]

$$\boldsymbol{\tau = 1.499/(f_0\, E^2)} \qquad (3.1)$$

where E is the excitation energy in cm^{-1} and f_0 is the oscillator strength of the excited state. Using Eq. (3.1) we have calculated radiative life time of all the five compounds which are listed in the Table 3.2.

Table 3.2. Calculated emission wavelength (in nm) (electronic transition $S_1 \rightarrow S_0$), the oscillator strength (*f*), orbital contribution, and emission energies (in eV) of difluoroboron napthyridine molecule at the TD-B3LYP/6-311+G (d) level of theory.

Molecules	Emission wavelength (nm)	Oscillator strength (*f*)	Orbital contribution (HOMO-LUMO)		Stokes Shift (nm)	τ (ns)
A(Gas)	400 (3.0974 eV)	0.199	H→L	0.6916	36	9.18
	324 (3.8304 eV)	0.001	H-2→L	0.6907	6	
A(DCM)	421(2.9422 eV)	0.406	H→L	0.6472	49	3.15
B(Gas)	420 (2.9429 eV)	0.271	H→L	0.6942	64	8.65
	319 (3.8943 eV)	0.004	H-2→L	0.6621	9	
B(DCM)	459 (2.5496 eV)	0.354	H-1→L	0.6450	94	5.57
C(Gas)	416(2.9827 eV)	0.298	H→L	0.7011	43	6.87
C(DCM)	439(2.8249eV)	0.459	H→L	0.7034	65	4.19
D(Gas)	421 (2.9421 eV)	0.202	H→L	0.6414	53	8.02
	323 (3.8328 eV)	0.002	H-2→L	0.6734	7	
D(DCM)	463 (2.5476 eV)	0.418	H→L	0.6887	87	5.15
E(Gas)	455 (2.7231 eV)	0.169	H→L	0.6942	79	8.99
	321 (3.8584 eV)	0.004	H-2→L	0.6252	14	
E((DCM)	477 (2.0249 eV)	0.305	H→L	0.6916	98	5.33

3.3.5. Frontier molecular orbitals

Effect of spectroscopic properties with the change in solvent behavior in the difluoroboron napthyridine can be explained by scrutinizing the difference between HOMO and LUMO. Frontier molecular orbital (FMO) is very useful to get information about excitation properties of organic molecules.[51],[52] The FMO energy levels along with

the HOMO–LUMO gaps are depicted in Fig. 3.5. Among these five molecules, compound B has highest HOMO-LUMO gap 3.90 eV whereas the compound E has lowest HOMO-LUMO gap which reveal that with the introduction of π-donating group such as methyl and amino into the difluoroboron napthyridine moiety the HOMO-LUMO gap decreases. As π conjugation increases from B to C in electron withdrawing substituents, the HOMO-LUMO gap decreases from 3.90 eV to 3.83 eV in vacuum. Compound D which has positive inductive effect shows HOMO-LUMO gap 3.77 eV, which is further reduced to 3.69 eV in compound E having strong resonance effect. Also from absorption and emission spectral values we find that compound E has interesting photo-physical properties. This indicates that those molecules which have small HOMO-LUMO gap, show higher absorption and emission wavelengths which is important for optoelectronic applications. FMO energy level diagrams of the molecules show that LUMO orbitals in polar solvent are more stabilized than HOMO orbitals. The energy difference between HOMO and LUMO in DCM, i.e., in polar solvent is low compared to that in the gas phase. It demonstrates that the LUMO orbital is more stabilized in polar environment than non-polar environment. This justifies the red shift which we observe in polar solvent. The plots of HOMO and LUMO of compound E is shown in Fig. 3.6 and other plots are in supporting information (Fig. S3 to S6) have isovalue 0.02. In case of compound E, it is clearly found from the HOMO-LUMO plot that both HOMO and LUMO orbitals (Fig. 3.6) are more diffused and electrons are more spread out among degenerate orbitals in solvent phase than in gas phase. For all the molecules napthyridine unit is mainly involved in the stabilization of HOMO -1 orbital in both phases.

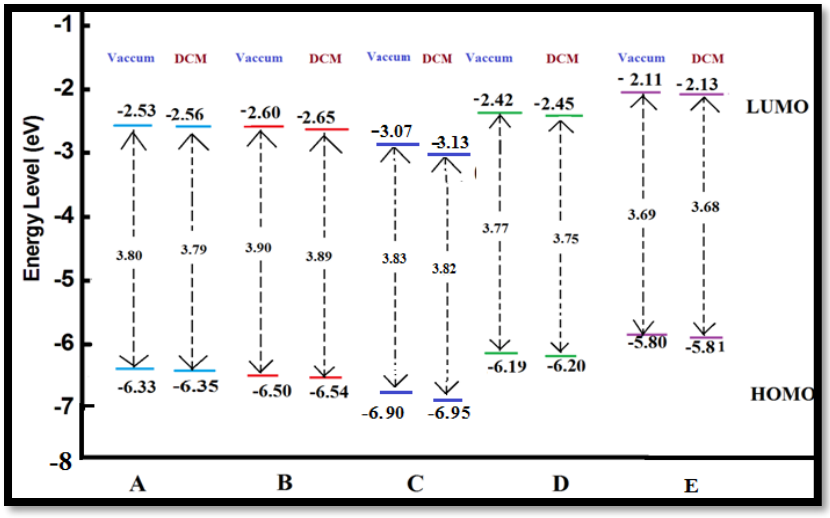

Fig. 3.5. Frontier Molecular Orbital (FMO) energy level diagram of the difluoroboron napthyridine molecules in gas phase and in dichloromethane solvent (DCM).

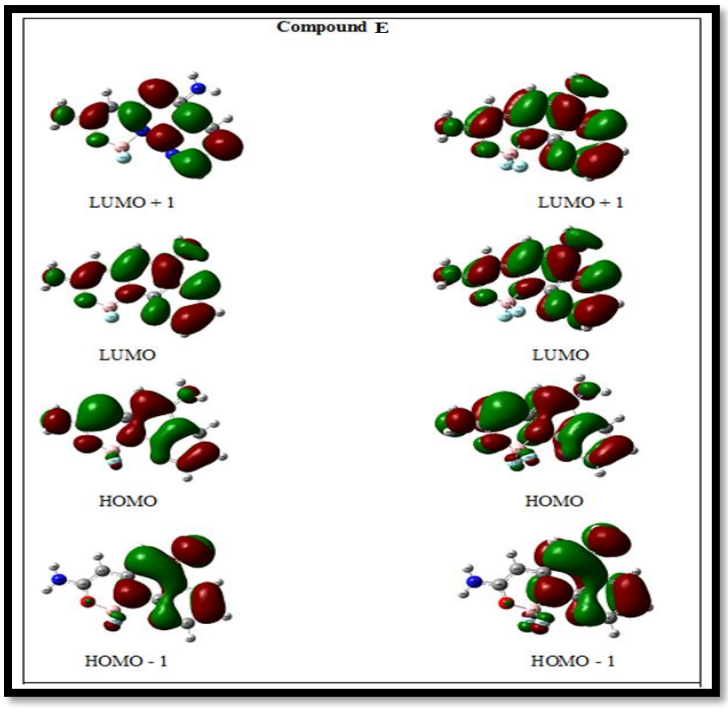

Fig. 3.6. Frontier molecular orbitals of the molecule BF_2 - napthyridine derivative (E) in gas phase (left panel) and in DCM (right panel).

3.3.6. Ionization potential and electron affinity

Ionization potentials (IPs) and electron affinities (EAs) of organic molecules are important properties which give information about the charge-injection and charge-transport character of a molecule. The adiabatic IP and EA are calculated at B3LYP/6-311+G (d) as well as with CAM-B3LYP[53] functional with 6-311+G (d) basis set to include long range correction for improving the charge transport that the B3LYP functional underrate enormously.[54] For understanding charge transfer characteristics better, range separated hybrid functional like CAM-B3LYP needs to be used rather than the B3LYP. In following discussion the results have been considered using CAM-B3LYP functional. Charge transport estimates the energy barrier for the injection of both electrons and holes into the compound. High EA of conjugated molecule for improving the electron injection/transport and low IP of conjugated molecules for better hole injection/transport is main key for the achievement of OLED. The calculated results are listed in Table 3.3, where we observed that for compound E, the energy required to create a hole is around 7.22 eV, which is lower than the other molecules. The result suggests that the hole injection and transportation of amino substituted group is easier than others. The order of IP is C > B > A > D > E, ionization potential decreases from electron withdrawing group to electron donating group. The presence of amino group in the BF_2-napthyridine moiety makes energy of HOMO higher which is similar from the result obtained from Lin et al.[55] Results found using B3LYP and CAM- B3LYP functionals follow the same trend.

On the other hand, the compound C has highest EA value (1.79 eV). We can say that it is easier to transport electron from C than other compounds. It is clear from Table 3.3 that compound E hold lower EA value and was found to exhibit higher hole transport property and poor electron transport ability. This is also reflected in λ_{hole} value which is discussed later. Whereas compound C hold highest EA and IP value and reveal good electron transport ability. It is interesting to mention that the lower HOMO-LUMO gap in compound E show minimum IP value, this indicates compound E can be used as hole transport material. Thus, this study shows that the introduction of electron donating group

make BF_2-napthyridine complex as more hole transporting material and electron withdrawing group make BF_2-napthyridine complex as more electron transporting material.

Table 3.3. Calculated ionization potentials (IPs in eV), electron affinities (EAs in eV), reorganization energies (eV) for hole (λ_{hole}) and electron ($\lambda_{electron}$) of the BF_2-napthyridine molecules (A to E). Calculations are done by applying adiabatic condition.

	IP		EA		λ_{hole}		$\lambda_{electron}$	
System	**B3 LYP**	**CAM-B3LYP**	**B3LYP**	**CAM-B3LYP**	**B3LYP**	**CAM-B3LYP**	**B3LYP**	**CAM-B3LYP**
A	7.78	7.89	1.17	1.14	0.452	0.544	0.381	0.489
B	7.91	8.01	1.26	1.24	0.489	0.598	0.440	0.544
C	8.11	8.21	1.89	1.79	0.465	0.571	0.489	0.652
D	7.58	7.67	1.09	1.06	0.448	0.543	0.386	0.491
E	7.14	7.22	0.86	0.83	0.444	0.462	0.544	0.653

3.3.7. Reorganization energy

In organic molecules charge mobility is described by hopping model. Marcus theory[56-58] is used for the account of inter-molecular charge transfer of hole and electron given in the following equation:

$$K_{et} = A \exp\left[\frac{-\lambda}{4K_bT}\right] \qquad (3.2)$$

where T is temperature, A is a prefactor related to the electron coupling between adjacent molecules, λ is the reorganization energies, and k_b is the Boltzmann constant. For an efficient charge transport, the reorganization energy (λ_{hole} or $\lambda_{electron}$) need to be small. It is important to remember that the lower the hole transport reorganization energy (λ_{hole}), the molecule act as better hole transport material (HTM). Likewise, the lower the electron transport reorganization energy ($\lambda_{electron}$) the molecule show faster electron transport property. λ_{hole} is sum of two contribution $\lambda_1 + \lambda_2$ are defined as:

$$\lambda_{hole} = \lambda_1 + \lambda_2 = [\, E_0(M^+) - E_0\,(M^*)] + [E_1(M^*) - E_1\,(M^+)] \qquad (3.3)$$

Where $E_0(M^+)$ and $E_0\,(M^*)$ represent the energies of neutral molecule at cation geometry and ground state energy of neutral molecule. Similarly, the reorganization energy for electron transfer, $\lambda_{electron}$ can be expressed by the sum of two contributions $\lambda_3 + \lambda_4$ as follows:

$$\lambda_{electron} = \lambda_3 + \lambda_4 = [\, E_0(M^-) - E_0\,(M^*)] + [E_1(M^*) - E_1\,(M^-)] \qquad (3.4)$$

Where $E_0\,(M^-)$ and $E_0\,(M^*)$ represent energy of the neutral molecule at the anion geometry and ground state energy of neutral molecule. The calculated reorganization energy for hole and electron are listed in Table 3.3 which exhibits that compound E is the best hole transport material and A is the best electron transport material. The difference between λ_{hole} and $\lambda_{electron}$ of all the compounds in B3LYP functional are less than 0.15 eV, suggest that they can act as emitter with moderately high light–emitting efficiencies.[59] The $\lambda_{electron}$ for compound A is smaller than its λ_{hole}, this indicate that the electron transfer rate is higher than the hole transfer rate. This case is just the contrary in compound E due to smaller λ_{hole} than $\lambda_{electron}$. By comparing reorganization energy values, we observed that with the introduction of electron donating groups, hole transport property increases. Overall, these molecules are good hole and electron transport material and can be adjusted upon suitable substitution.

3. 4. Conclusions

In this work, we report a theoretical study to gain more information on the optoelectronic properties of five difluoroboron-napthyridine analogs through DFT and TD-DFT study. All compounds were subjected to UV–Vis absorption and fluorescence studies in gas phase and in dichloromethane and the results have been interpreted. The photophysical properties of the five compounds are successfully assessed using absorption and emission spectroscopy. It is found that absorption profile is slightly changed by the solvent whereas fluorescence profile is greatly affected by solvent. As expected, red shift is found in absorption and emission spectra with increasing electron

delocalization. It is evident from this study that amine substituted BF_2 napthyridine complex has lowest HOMO-LUMO energy gap and largest Stokes shift in gas phase as well as in solution phase. For emission spectra of A to E compounds, decreasing electron accepting strength and with increasing electron donating ability outcomes red shifted emission. The emission property of amine substituted BF_2-napthyridine established high photoluminescence property compared to other molecules. The FMO analysis shows that HOMO and LUMO orbitals are more stabilized in polar environment. Napthyridine ring also play a vital role in electron density delocalization and to enhance optical phenomena. The calculated reorganization energy suggest that compound E and A can be used as HTM and ETM. In conclusion, the results reveal that difluoroboron complexes show significant photoluminescence behavior with the change of substitution in the ketoiminate position. This outcome provides a practical direction towards fluorescent difluoroboron napthyridine complexes for application in organic luminescence materials, biological sensing, and self illuminating fluorescence for in vivo studies.

3.5. References

1. Tanaka, K.; Chujo, Y., *Npg Asia Mater.*, **2015**, *7*, e223.
2. Entwistle, C. D.; Marder, T. B., *Angew. Chem. Int. Ed.*, **2002**, *41* (*16*), 2927-2931.
3. Plesek, J., *Chem. Rev.* **1992**, *92* (2), 269-278.
4. Frath, D.; Poirel, A.; Ulrich, G.; De Nicola, A.; Ziessel, R., *Chem. Commun.*, **2013**, *49* (43), 4908-4910.
5. Frath, D.; Massue, J.; Ulrich, G.; Ziessel, R., *Angew. Chem. Int. Ed.*, **2014**, *53* (9), 2290-2310.
6. Cheng, F.; Jäkle, F., *Chem. Comm.*, **2010**, *46* (21), 3717-3719.
7. Kubota, Y.; Ozaki, Y.; Funabiki, K.; Matsui, M., *J. Org. Chem.*, **2013**, *78* (14), 7058-7067.
8. Liao, C.-W.; Rao, R.; Sun, S.-S., *Chem. Comm.*, **2015**, *51* (13), 2656-2659.
9. Ono, K.; Hashizume, J.; Yamaguchi, H.; Tomura, M.; Nishida, J.-I.; Yamashita, Y., *Org. Lett.*, **2009**, *11* (19), 4326-4329.
10. Ośmiałowski, B.; Zakrzewska, A.; Jedrzejewska, B.; Grabarz, A.; Zaleśny, R.; Bartkowiak, W.; Kolehmainen, E., *J. Org. Chem.*, **2015**, *80* (4), 2072-2080.
11. Zakrzewska, A.; Zaleśny, R.; Kolehmainen, E.; Ośmiałowski, B.; Jędrzejewska, B.; Ågren, H.; Pietrzak, M., *Dyes Pigm.* ,**2013**, *99* (3), 957-965.
12. Fischer, G. M.; Ehlers, A. P.; Zumbusch, A.; Daltrozzo, E., *Angew. Chem. Int. Ed.*, **2007**, *46* (20), 3750-3753.
13. Fischer, G. M.; Isomäki-Krondahl, M.; Göttker-Schnetmann, I.; Daltrozzo, E.; Zumbusch, A., *Chem. Eur. J.*, **2009**, *15* (19), 4857-4864.

14. Erten-Ela, S.; Yilmaz, M. D.; Icli, B.; Dede, Y.; Icli, S.; Akkaya, E. U., *Org. Lett*., **2008**, *10* (15), 3299-3302.
15. Fan, G.; Yang, L.; Chen, Z., *Front. Chem. Sci. Eng.*, **2014**, *8* (4), 405-417.
16. Brabec, C. J.; Sariciftci, N. S.; Hummelen, J. C., *Adv. Funct. Mater.*, **2001**, *11* (1), 15-26.
17. Mitschke, U.; Bäuerle, P., *J. Mater. Chem.*, **2000**, *10* (7), 1471-1507.
18. Komatsu, T.; Oushiki, D.; Takeda, A.; Miyamura, M.; Ueno, T.; Terai, T.; Hanaoka, K.; Urano, Y.; Mineno, T.; Nagano, T., *Chem. Comm.*, **2011**, *47* (36), 10055-10057.
19. Nepomnyashchii, A. B.; Bröring, M.; Ahrens, J.; Bard, A. J., *J. Am. Chem. Soc.*, **2011**, *133* (22), 8633-8645.
20. Bonardi, L.; Kanaan, H.; Camerel, F.; Jolinat, P.; Retailleau, P.; Ziessel, R., *Adv. Funct. Mater.*, **2008**, *18* (3), 401-413.
21. Kumaresan, D.; Thummel, R. P.; Bura, T.; Ulrich, G.; Ziessel, R., *Chem. Eur. J.*, **2009**, 15 (26), 6335-6339.
22. Lee, C. Y.; Hupp, J. T., *Langmuir*, **2010**, *26* (5), 3760-3765.
23. Lorenz-Rothe, M.; Schellhammer, K. S.; Jägeler-Hoheisel, T.; Meerheim, R.; Kraner, S.; Hein, M. P.; Schünemann, C.; Tietze, M. L.; Hummert, M.; Ortmann, F., *Adv. Electr. Mater.*, **2016**, 2 (10).
24. Singh, S. P.; Pavan Kumar, C.; Sharma, G.; Mikroyannidis, J.; Singh, M.; Kurchania, R., *J. Polym. Sci. B Polym. Phys*., **2012**, *50* (23), 1612-1618.
25. Zhou, Y.; Kim, J. W.; Kim, M. J.; Son, W.-J.; Han, S. J.; Kim, H. N.; Han, S.; Kim, Y.; Lee, C.; Kim, S.-J., *Org. Lett.*, **2010**, *12* (6), 1272-1275.
26. Contreras, J.; Xie, J.; Chen, Y. J.; Pei, H.; Zhang, G.; Fraser, C. L.; Hamm-Alvarez, S. F., *ACS Nano*, **2010**, *4* (5), 2735-2747.
27. Nakatani, K.; Horie, S.; Saito, I., *J. Am. Chem. Soc*,. **2003**, *125* (30), 8972-8973.
28. Hikishima, S.; Minakawa, N.; Kuramoto, K.; Fujisawa, Y.; Ogawa, M.; Matsuda, A., *Angew. Chem.*, **2005**, *117* (4), 602-604.
29. Katz, J. L.; Geller, B. J.; Foster, P. D., *Chem.Comm.*, **2007**, (10), 1026-1028.
30. Srivastava, S. K.; Jaggi, M.; Singh, A. T.; Madan, A.; Rani, N.; Vishnoi, M.; Agarwal, S. K.; Mukherjee, R.; Burman, A. C., *Bioorganic Med. Chem. Lett.*, **2007**, *17* (23), 6660-6664.
31. Egawa, H.; Miyamoto, T.; Minamida, A.; Nishimura, Y.; Okada, H.; Uno, H.; Matsumoto, J., *J. Med. Chem.*, **1984**, *27* (12), 1543-1548.
32. Lesher, G. Y.; Froelich, E. J.; Gruett, M. D.; Bailey, J. H.; Brundage, R. P., *J. Med. Pharm. Chem.*, **1962**, *5* (5), 1063-1065.
33. Fu, L.; Feng, X.; Wang, J.-J.; Xun, Z.; Hu, J.-D.; Zhang, J.-J.; Zhao, Y.-W.; Huang, Z.-B.; Shi, D.-Q., *ACS Comb. Sci.*, **2014**, *17* (1), 24-31.
34. Roma, G.; Di Braccio, M.; Grossi, G.; Mattioli, F.; Ghia, M. *Eur., J. Med. Chem*,. ***2000***, *35* (11), 1021-1035.
35. Sato, Y.; Seino, T.; Nishizawa, S.; Teramae, N., *Nucleic Acids Symp. Ser*., Oxford University Press: **2007**; pp 313-314.
36. Sato, Y.; Nishizawa, S.; Yoshimoto, K.; Seino, T.; Ichihashi, T.; Morita, K.; Teramae, N., *Nucleic Acids Res., **2009**, 37* (5), 1411-1422.
37. Fang, J.-M.; Selvi, S.; Liao, J.-H.; Slanina, Z.; Chen, C.-T.; Chou, P.-T., *J. Am. Chem. Soc.*, **2004**, *126* (11), 3559-3566.

38. Chen, Y.; Fu, W.-F.; Li, J.-L.; Zhao, X.-J.; Ou, X.-M., *New J. Chem.,* **2007**, *31* (10), 1785-1788.
39. Li, H.-J.; Fu, W.-F.; Li, L.; Gan, X.; Mu, W.-H.; Chen, W.-Q.; Duan, X.-M.; Song, H.-B., *Org. Lett,*. **2010**, *12* (13), 2924-2927.
40. Christie, R. M., Colour chemistry. *RSC*: **2001**.1-11
41. Frisch, M.; Trucks, G.; Schlegel, H. B.; Scuseria, G.; Robb, M.; Cheeseman, J.; Scalmani, G.; Barone, V.; Mennucci, B.; Petersson, G., et al. *Gaussian 09*, revision A. 02, gaussian. Inc., Wallingford, CT **2009**.
42. Feng, L.-Y.; Zhai, H.-J., *Phys. Chem. Chem. Phys.*, **2017**, *19* (35), 24284-24293.
43. Cossi, M.; Barone, V.; Cammi, R.; Tomasi, J., *Chem. Phys. Lett.*, **1996**, *255* (4-6), 327-335.
44. Tomasi, J.; Mennucci, B.; Cammi, R., *Chem. Rev.*, **2005**, *105* (8), 2999-3094.
45. Hachiya, S.; Inagaki, T.; Hashizume, D.; Maki, S.; Niwa, H.; Hirano, T., *Tetrahedron Lett.,* **2010**, *51* (12), 1613-1615.
46. Li, D.; Zhang, H.; Wang, C.; Huang, S.; Guo, J.; Wang, Y., *J. Mater. Chem.*, **2012**, *22* (10), 4319-4328.
47. Macedo, F. P.; Gwengo, C.; Lindeman, S. V.; Smith, M. D.; Gardinier, J. R., *Eur. J. Inorg. Chem.*, **2008,** *2008* (20), 3200-3211.
48. Chow, Y. L.; Wang, S.-S.; Cheng, X.-E., *Can. J. Chem.*, **1993**, *71* (6), 846-854.
49. Chow, Y. L.; Ouyang, X., *Can. J. Chem.*, **1991**, *69* (3), 423-431.
50. Chaitanya, K.; Ju, X.-H.; Heron, B. M. , *RSC Adv.*, **2014**, *4* (51), 26621-26634.
51. Solomon, R. V.; Veerapandian, P.; Vedha, S. A.; Venuvanalingam, P., *J. Phys. Chem. A*, **2012**, *116* (18), 4667-4677.
52. Gajalakshmi, D.; Solomon, R. V.; Tamilmani, V.; Boobalan, M.; Venuvanalingam, P., *RSC Adv.*, **2015**, *5* (62), 50353-50364.
53. Yanai, T.; Tew, D. P.; Handy, N. C., *Chem. Phys. Lett.*, **2004,** *393* (1-3), 51-57.
54. Asada, T.; Koseki, S., *Org. Electron,* **2018,** *53*, 141-150.
55. Lin, B. C.; Cheng, C. P.; Lao, Z. P. M., *J. Phys. Chem. A,* **2003**, *107* (26), 5241-5251.
56. Marcus, R. A. I., *J. Chem. Phys.* **1956**, *24* (5), 966-978.
57. Marcus, R. A. *Rev. Mod. Phys.*, **1993**, *65* (3), 599.
58. Liao, Y.; Yang, G.-C.; Feng, J.-K.; Shi, L.-L.; Yang, S.-Y.; Yang, L.; Ren, A.-M., *J. Phys. Chem. A,* **2006**, *110* (48), 13036-13044.
59. Zou, L.-Y.; Zhang, Z.-L.; Ren, A.-M.; Ran, X.-Q.; Feng, J.-K., *Theor. Chem. Acc.*, **2010**, *126* (5-6), 361-369.